Antibiotic-induced DNA damage results in a controlled loss of pH homeostasis and genome instability

James Alexander Booth,[1,6] Mário Špírek,[2, 4] Tekle Airgecho Lobie,[1] Kirsten Skarstad,[1] Lumir Krejci,[2,3,4,7] and Magnar Bjørås[1,5,6,7]

[1]Department of Microbiology, University of Oslo and Oslo University Hospital, Rikshospitalet, Oslo, Norway

[2]Department of Biology, Masaryk University, Kamenice 5/A7, CZ-62500 Brno, Czech Republic

[3]National Centre for Biomolecular Research, Masaryk University, Kamenice 5/A4, CZ-62500 Brno, Czech Republic

[4]International Clinical Research Center, Center for Biomolecular and Cellular Engineering, St. Anne's University Hospital Brno, Pekarska 53, CZ-656 91 Brno, Czech Republic

[5]Department of Cancer Research and Molecular Medicine, Norwegian University of Science and Technology, Trondheim, Norway.

[6]Corresponding Authors (james.booth@rr-research.no & magnar.bjoras@rr-research.no)

[7]Contributed equally

1

22 **ABSTRACT**

23 Extracellular pH has been assumed to play little if any role in how bacteria respond to

24 antibiotics and antibiotic resistance development. Here, we show that the intracellular

25 pH of *Escherichia coli* equilibrates to the environmental pH following antibiotic

26 treatment. We demonstrate that this allows the environmental pH to influence the

27 transcription of various DNA damage response genes and physiological processes

28 such as filamentation. Using purified RecA and a known pH-sensitive mutant variant

29 RecA K250R we show how pH can affect the biochemical activity of a protein central

30 to control of the bacterial DNA damage response system. Finally, two different

31 mutagenesis assays indicate that environmental pH affects antibiotic resistance

32 development. Specifically, at environmental pH's greater than six we find that

33 mutagenesis plays a significant role in producing antibiotic resistant mutants. At pH's

34 less than or equal to 6 the genome appears more stable but extensive filamentation is

35 observed, a phenomenon that has previously been linked to increased survival in the

36 presence of macrophages.

37

INTRODUCTION

There is considerable medical concern about the rise in antibiotic-resistant infections (1). Recalcitrance to treatment has been shown to occur due to mutagenesis or mechanisms of transitory tolerance and persistence (2). Antibiotic treatment can lead to DNA damage, genomic instability and subsequently accelerated resistance development in bacteria. As a consequence of DNA damage the bacterial SOS response is induced (3,4). The SOS response (SOS) encompasses over 50 genes with several linked to antibiotic resistance development (5,6). SOS has several physiological effects including the depolarisation of the electrical potential difference ($\Delta\Psi$) across the inner membrane of the bacterium (7-9). $\Delta\Psi$ quantifies the difference in charge across a membrane and is one of two components that make up the proton motive force (pmf). The proton gradient (ΔpH), the other component of the pmf varies as the external pH changes and pH homeostasis maintains the intracellular pH within a narrow range of ~7.5-7.7 (10,11). As bacteria such as *Escherichia coli* (*E. coli*) have a permissive proliferation pH range of 5-9 both $\Delta\Psi$ and ΔpH have to be actively managed to maintain pmf and pH homeostasis (10).

Here, we wished to test if antibiotic treatment of *E. coli* would affect the ΔpH and to understand the consequences of these changes. First we demonstrated that the quinolone antibiotic, nalidixic acid, induces a *recA*-dependent controlled loss of ΔpH. As a consequence we show the changes in intracellular pH result in alterations in the biochemical activities of RecA, including recombination and strength of transcription of various SOS response genes. Additionally, filamentation, rates of mutagenesis and viability were also shown to be dependent on the external pH. Our results thus show that the pH of the external environment affects how the bacterium reacts to antibiotics

3

62   and demonstrates that *E. coli* uses different antibiotic survival strategies at different

63   pH's.

64

MATERIAL AND METHODS

Strains and microbial techniques

67   Unless otherwise stated the wild type *E. coli* MG1655 strain was used. Bacterial

68   strains and plasmids used are listed in Supplementary Table S1. The *recA* mutant was

69   generated from the keio collection and transduced into MG1655 (12). Transfer of

70   genotypes of interest was carried out by P1 transduction (13). Transformation of

71   plasmids was carried out using electroporation using electrocompetent cells generated

72   using a glycerol/mannitol density step centrifugation (14). Genetic antibiotic selection

73   markers flanked by FRT sites were removed using the FLP recombinase containing

74   plasmid pCP20 (15). Antibiotics were used at the following concentrations,

75   kanamycin 50 µg/ml (plasmid selection) 30 µg/ml (genomic selection), ampicillin 100

76   µg/ml (plasmid selection) and nalidixic acid 100 µg/ml (optimum concentration for

77   lethality) (16). LB broth (10 g tryptone, 5 g yeast extract, 10 g NaCl adjusted to 1 l

78   with MQ H_2O and autoclaved) was used for none pH adjusted experiments together

79   with agar (1.5%) if for solid media. LBK (10 g tryptone, 5 g yeast extract, 7.45 g KCl,

80   adjusted to 1 l with MQ H_2O and autoclaved) was used to limit the sodium ion

81   concentrations, which inhibit growth at high pH. M9 minimum glycerol media was

82   prepared by diluting sterile (M9 (10x) 100 ml, $MgSO_4$ (1 M) 1 ml, $CaCl_2$ (0.2 M) 2

83   ml, thiamine (5%) 2 ml and glycerol (60%) 1.67 ml) into pre-autoclaved MQ H_2O to

84   1 l, containing 15 g agar (1.5%) if for plates. M9 minimum lactose media was

85   prepared as mentioned above by substituting lactose (20%, 50.1 ml) for glycerol. The

86   pH's of LBK, M9 minimal media and PBS solutions were adjusted (100 mM) with

87   Good's sulfonate buffers, 2-(N-Morpholino)ethanesulfonic acid hydrate (MES) for

88   pH's 5.2, 5.5 and 6, 3-(N-Morpholino)propanesulfonic acid (MOPS) for pH 7 and N-

5

89   [Tris(hydroxymethyl)methyl]-3-aminopropanesulfonic acid (TAPS) for pH 8.

90   Adjustments were carried out with KOH (5 M) and the solutions sterilised by

91   filtration (0.2 µm).

92   **Survival assay – Nalidixic acid**

93   Acute survival was measured by survival following the removal of the DNA

94   damage induced by nalidixic acid. The strains were grown (37°C, 200 rpm) in

95   quadruplet in media (LB or pH adjusted LBK, 3 ml in a 15 ml tube) to OD_{600}=0.8.

96   The first sample was taken before addition of nalidixic acid and designated as t=0.

97   Samples were centrifuged (21,500 g, 20 s) media aspirated and the pellet re-

98   suspended (PBS) to remove the nalidixic acid. The samples were then serially diluted

99   (10x, 100 µl, PBS or pH adjusted PBS) in 96 well plates before samples (10 µl) were

100   transferred to 24 well plates containing only LB-agar or pH adjusted LBK-agar (1

101   ml/well, 1.5% agar). The droplets were allowed to dry, then incubated (overnight,

102   37°C) in the dark before enumeration the following day. For each sample the well

103   containing 10-100 colonies was counted and used to calculate CFU/ml. Samples were

104   taken at the time points indicated on the graphs.

105   **Flow cytometry – Intracellualar pH determination**

106   The strains were grown (37°C, 200 rpm) in quadruplet in pH adjusted media

107   (LBK, 3 ml in a 15 ml tube) containing 200 µM arabinose to OD_{600}=0.8 (Nanodrop,

108   ND-1000). The arabinose maintains high levels of expression and keeps the majority

109   of active GFP in the cytoplasm (17). The first sample was taken before addition of

110   nalidixic acid and designated as t=0. The samples (2 µl) were diluted into several pH

111   buffered PBS solutions (100 µl), one at the pH of the LBK and a calibration curve of

112   five pH buffered PBS solutions containing the membrane permeable weak acid

113   sodium benzoate (60 mM). Benzoate collapses the ΔpH across the inner membrane

114   resulting in the internal pH equalization to that of the external solution. The

115   extracellular pH's were chosen to ensure that at least one of the solutions was higher

116   and one was lower in pH compared to the intracellular pH of the bacteria. The

117   fluorescence signal of the TorA-GFPmut3* protein from 10,000 bacteria/sample was

118   then measured on an AccuriC6 flow cytometer in FLA-1. Subsequent samples were

119   taken at the time points indicated after exposure to nalidixic acid. The intracellular pH

120   values were calculated using the two solutions on the calibration curve that straddled

121   the fluorescence intensity value of the unknown LBK sample.

Flow cytometry - SOS induction and *recA, lexA & umuDC-gfp* measurement

123   The strains were grown (37^oC, 200 rpm) in quadruplet in pH adjusted media

124   (LBK, 3 ml in a 15 ml tube) to OD_{600}=0.8 (Nanodrop, ND-1000). The first sample

125   was taken before addition of nalidixic acid and designated as t=0. The samples (2 µl)

126   were diluted into PBS (100 µl) buffered to the same pH as the incubating media and

127   simultaneously at pH 8 supplemented with sodium benzoate (60 mM) at room

128   temperature. The GFP signal is maximised and standardised by using PBS at pH 8

129   together with sodium benzoate (60 mM) and eliminates the GFP signal fluctuations

130   due to the pH variations due to the pH equilibration. The fluorescence signal from

131   10,000 bacteria/sample from the GFPmut2 protein or the RecA-GFP fusion, where the

132   GFP moiety is Gfp-901, a derivative of GFPmut2, were measured on an AccuriC6

133   flow cytometer in FLA-1. Subsequent samples were taken at the time points indicated

134   after exposure to nalidixic acid.

135   **Electromobility shift assay (EMSA)**

136   The EMSA described is a modification of a previously published protocol (18).

137   RecA was diluted from concentrated stock (New England Biolabs M0249L) into

138   Storage Buffer (50 mM phosphate/citrate buffer at pH 7, 50 mM NaCl), which was

139   also used in no protein control. Protein was mixed with a master mix (containing 900

140   nM (nucleotides) 5'-FITC-labelled 90mer oligonucleotide

141   (AAATCAATCTAAAGTATATATGAGTAAACTTGGTCTGACAGTTACCAATG

142   CTTAATCAGTGAGGCACCTATCTCAGCGATCTGTCTATTT), 50 mM

143   phosphate/citrate buffer at pH 5 to 8, 50 mM NaCl, 10 mM $MgCl_2$ and 1 mM ATP)

144   according to the indicated scheme in 10 μl reaction volume at 25°C for 5 minutes. The

145   reactions were stopped by addition of glutaraldehyde to final concentration of 0.125%

146   for additional 5 minutes and then transferred to ice. Reactions were resolved on 1%

147   agarose gels in 1X TAE (70 V, 2 h). Gels were subjected to fluorescent analysis and

148   data quantification using the FLA-9000 Starion (Fujifilm) and MultiGauge (Fujifilm)

149   software.

D-loop formation assays

151   The reaction was performed as described earlier (19). Briefly, RecA was

152   incubated for 5 min with 50 nM (moles) 5'-FITC-labelled 90mer oligonucleotide as in

153   the EMSA experiment and 2 μl (920 ng) of pBluescript SK(–) (460 ng/μl) was then

154   added to bring the final reaction volume to 10 μl and incubated for 10 min at 37 °C.

155   The samples were deproteinized with 0.1% SDS and 10 μg proteinase K for 10 min at

156   37°C and resolved in 0.9% agarose gels in 1X TAE (90 V, 35 min). Gels were imaged

157   on a FLA-9000 scanner (Fujifilm) and quantified with Multi Gauge V3.2 (Fujifilm).

Stopped-flow assays and data analysis

159   The experiments were performed essential as described previously using an

160   SFM-300 stopped-flow machine (Bio-Logic) fitted with a MOS-200 monochromator

161   spectrometer (Bio-Logic) with excitation wavelength set at 545 nm(20). Fluorescence

162   measurements were collected with a 550 nm long pass emission filter. The machine

163   temperature was maintained at 25°C with a circulating water bath. For all

164   experimental setups, a master mix containing all common reaction components for

165   each of the two syringes was prepared. To these mixtures a variable RecA amounts

166   were added. Since equal volumes were injected into the mixing chamber from each

167   syringe, the two solutions became mutually diluted. Therefore, all reaction

168   components common to each syringe were prepared at the final concentration,

169   whereas reaction components present in only one syringe were added at twice the

170   desired final concentration. All concentrations quoted represent final concentrations

171   after mixing. Components of each syringe were pre-incubated for 10 min before the

172   start of experiments to allow the contents to reach equilibrium.

173   All reactions were performed in Stopped Flow Buffer (50 mM phosphate/citrate

174   buffer (pH 5 to 8), 10 mM $MgCl_2$, 50 mM NaCl, 1 mM ATP). All reactions contained

175   20 nM 5'-Cy3 fluorescently labelled (dT79). RecA was added directly from

176   concentrated stocks. For all experiments, control reactions were also performed for

177   buffer alone with and without DNA to confirm fluorescence signal stability over the

178   time course of the experiments (data not shown).

179   Fluorescence measurements for most experiments were collected according to

180   the following protocol: (1) every 0.00005 s from 0-0.05 s; (2) every 0.0005 s from

181   0.05-0.56 s; (3) every 0.02 s from 0.56-120.54 s. For each condition analysed, traces

182   were collected from between three and nine independent reactions (n = 3-9) and

183   averages were generated. Importantly, all conclusions from this study are made on the

184   magnitude and rate of changes in fluorescence over time and how these vary with

185   RecA concentration, and therefore the absolute fluorescence values were converted to

186   arbitrary units by a normalisation procedure to facilitate comparison. For all

187   experiments the raw data were normalised to the same fluorescence value for the 0 s

188   time point.

189   For analysis, for all experiments ten-point moving averages were calculated on

190   each individual normalised trace, which were used to define initial (0 s), final (120.54

191   s) and maximum fluorescence (and corresponding time point), and ΔCy3 fluorescence

192   values for each experiment. To simplify direct comparison of conditions for various

193   pH conditions we calculated observed overall half-times, measured from time points

194   where the fluorescence from moving averages was closest to the value calculated for

195   ΔCy3 fluorescence midpoints.

196   **LexA degradation assay**

197   RecA (0.6 μM) was mixed with ssDNA (30-mer, 70 nM) in citrate-phosphate buffer

198   with various pH containing 35 mM NaCl, 10 mM $MgCl_2$ and either 1 mM ATP or

199   ATPgammaS. RecA nucleofilaments were formed for 10 minutes at 37°C and then

200   mixed with LexA protein. Reactions were stopped at 0, 60 or 120 minutes by

201   addition of Laemmli buffer. Samples were resolved in 15% SDS-PAGE gels and

202   stained with Coomassie stain. The intensity of bands for full length LexA protein

203   were analysed by MultiGauge Software. The average signal is shown with standard

204   error for 3 independent experiments.

205   **Lactose reversion assay**

206   FC29 (Rif^S, F' Δ(*lacI lacZ*)) *E. coli* cannot utilise lactose as a carbon source or revert

207   from Lac⁻ to Lac⁺. FC40 (Rif^R, F' *lacIΩlacZ*) eliminates the coding sequence of the

10

208   last four residues of *lacI*, all of *lacP* and *lacO*, and the first 23 residues of *lacZ* (21).

209   Individual colonies on M9 minimum glycerol plates were used to seed M9 minimal

210   glycerol (30°C, 200 rpm, 1 ml in 15 ml tubes, three days). pH adjusted M9 minimum

211   lactose agar plates were inoculated with 10^{10} FC29 to scavenge each plate for sources

212   of carbon other than lactose. The next day, the plates were overlaid with 1:10

213   (FC29:FC40) suspended in pH adjusted M9 minimal lactose top agar (0.5% agar) and

214   incubated at 37°C.

215   The frequency of Lac$^+$ revertants was determined by counting Lac$^+$ colonies every 24

216   hours for 12 days and calculating the mean and standard deviation (n=3).

217   **MIC assay**

218   Wild type *E. coli* (*MG1655*) was grown overnight (37°C, LB agar plates) before being

219   resuspended in pH adjust LBK media and adjusted to an OD_{600}=0.03. The antibiotics

220   were dissolved to a final concentration of 128 µg/ml in pH adjusted LBK and serially

221   diluted (x2) to 0.25 µg/ml (giving 10 concentrations of each antibiotic). A single µl of

222   adjusted bacterial culture was added to each well (100 µl). The plates were then

223   incubated (37°C) and the OD_{595} read the following day. The experiments were

224   repeated in quadruplet to determine the mean and standard deviation.

225   **Forward UV induced rifampicin resistance assay**

226   pH adjusted PBS and LBK media were used throughout. Wild type *E. coli* (*MG1655*)

227   were grown overnight (37°C, 1.5% agar) before being diluted and resuspended

228   (<1000 bacteria / culture) in liquid media for overnight growth (37°C, 200 rpm). The

229   following day the bacteria were diluted (x50) and grown to OD_{600}=0.25 before being

230   centrifuged and resuspended in PBS and exposed to UV (20 J/m^2) or not.

231   Subsequently all cultures were kept in the dark. The samples of the cultures were then

11

232   plated on Rifampicin (100 µg/ml) plates and also on LBK to determine CFU. The

233   cultures were then centrifuged and resuspended in LBK before incubation (37°C, 200

234   rpm, ON). The following day the cultures were plated on Rifampicin (100 µg/ml) and

235   LBK to determine CFU. The following day the concentration of rifampicin resistant

236   bacteria was calculated. The mean and standard deviation were calculated from three

237   independent experiments.

238   **Bacterial viability assay with propidium iodide**

239   Bacteria were grown overnight (37°C, LB agar plates) before being resuspended in

240   pH adjust LBK media and adjusted to an OD_{600}=0.03. The strain(s) were grown

241   (37°C, 200 rpm) in pH adjusted media (LBK, 3 ml in a 15 ml tube) to OD_{600}=0.6

242   (Nanodrop, ND-1000). The first sample was taken before addition of nalidixic acid

243   and designated as t=0. The samples (2 µl) were diluted into PBS (100 µl) buffered to

244   the sample pH as the incubating media and containing PI (2 µl) in pairs where one of

245   the samples was also treated with EtOH (100 µl). The fluorescence signal of PI from

246   10,000 bacteria/sample were then measured on an AccuriC6 flow cytometer in FLA-

247   3. Simultaneous readings of FSC-A were recorded and used to calculate the density of

248   PI in the bacteria. Subsequent samples were taken at the time points indicated after

249   exposure to nalidixic acid. All experiments were run on at least three independent

250   days.

251

12

RESULTS

DNA damage leads to the loss of pH homeostasis

To induce DNA damage we used the antibiotic nalidixic acid a quinolone that binds

DNA gyrase and topoisomerase IV inhibiting their ligation activities leading to DNA

double strand breaks and chromosome fragmentation (22). To explore the hypothesis

that antibiotic-induced DNA damage affects the proton gradient of the bacterium we

first confirmed that nalidixic acid led to the *recA*-dependent loss of electrical potential

(Supplementary Figure S1 and Results) (23). Thereafter, we tested the potential of a

pH sensitive reporter, GFPmut3* (Supplementary Table S1), to follow intracellular

pH changes (Supplementary Figure S2) (24). *E. coli* expressing GFPmut3* were

grown to exponential phase before treating with Nalidixic acid (100 μg/ml). The

fluorescence of GFPmut3* was recorded by flow cytometry both before and after

treatment and simultaneously the GFPmut3* signal of each sample was calibrated

over the possible pH range. We observed that the calibration curve changed over time

following the introduction of the antibiotic and determined that continuous calibration

of GFPmut3* was necessary (Supplementary Figure S3). The intracellular pH of *E.*

coli was monitored for four hours following antibiotic-induced DNA damage where

the external pH was buffered to pH 7 (Figure 1A). Following a delay of 30 minutes,

the intracellular pH fell reaching the pH of the extracellular environment about 120

minutes after the addition of nalidixic acid.

E. coli is the predominant aerobic organism in the caecum and colon of the human

gastrointestinal tract where the pH varies from 5.7-6.8 and 6.1-7.2 respectively

(25,26). Additionally, pathogenesis can lead certain *E. coli* strains to be exposed to

the urinary tract (pH 4.5-8 (27)) and the eukaryotic intracellular environment which

includes macrophages and phagosomes (pH 5-7.5 (28)). Due to these various

13

277 ecological niches occupied by *E. coli*, we were curious as to how the external pH may

278 affect the kinetics of loss of proton homeostasis in more acidic environments.

279 Buffering the media to either pH 6 or 5.5 led to the decrease of intracellular pH to

280 almost that of the external media over 180-240 minutes (Figure 1A). As RecA

281 coordinates the DNA damage induced-stress response in *E. coli*, by inducing the

282 expression of LexA sensitive genes in a dose-dependent manner (29), we used a *recA*

283 mutant to demonstrate a significant reduction in proton depolarisation after treatment

284 with nalidixic acid as compared to wild type (Figure 1B). Additionally, we noted in

285 the wild type that electrical depolarisation never fully equilibrated at pH 7 whilst

286 proton equilibration was achieved after two hours. Identical experimental setups

287 allowed for a direct comparison illustrating that the two processes appear to be

288 kinetically independent (Figure 1C). Together these results show both $\Delta\Psi$ and ΔpH

289 equilibrate with their external environment in a *recA*-dependent manner. However, the

290 kinetics of equilibration indicate the two processes appear be independent of each

291 other.

External pH affects filamentation and *recA* transcription

293 The *recA* dependency of proton equilibration following DNA damage suggested that

294 various SOS processes may also be dependent on the external pH. Filamentation

295 following induction of the SOS response is a classical morphological response to

296 DNA damage (30-32). Therefore, we investigated if the external pH would influence

297 the dynamics and extent of filamentation following DNA damage using flow

298 cytometry by following forward scatter (FSC-A), as a proxy for cell volume(33).

299 Surprisingly, when the extracellular pH was buffered to pH 7 after exposure to

300 nalidixic acid cell filamentation showed an initial increase followed by a gradual

301 decline (Figure 2A). Next we examined how the external pH buffered to 6 or 5.5

14

302   would affect the dynamics of filamentation. Both pH conditions showed a greater

303   extent of filamentation (Figure 2A). These data demonstrate that following DNA

304   damage the external pH can affect internal cellular processes, such as filamentation

305   and loss of mean cell volume via changes in the intracellular pH.

306   As the expression of RecA is immediate following the introduction of a substantial

307   amount of DNA damage (34) we next examined the RecA-mediated transcriptional

308   SOS response over the replicative permissive pH range of *E. coli*. To monitor the

309   induction and kinetics of the SOS response we used a strain expressing an optimised

310   genomic *recA-gfpmut2* fusion protein which responds quickly to SOS induction and

311   minimizes steric interference of the tag (*recA-gfp*, Supplementary Table S1) (35). We

312   calculated GFP fluorescence density by dividing fluorescence (Supplementary Figure

313   S4A) by FSC-A (Supplementary Figure S4B) measurements to account for cell size

314   effects (Supplementary Results). Using an identical experimental setup as utilised to

315   determine the loss of pH homeostasis, the *recA-gfp* strain was grown to the

316   exponential phase before exposure to nalidixic acid in four different medias buffered

317   to pHs 5.2, 6, 7 and 8 (Figure 2B). pH 6 promoted the most substantial expression of

318   RecA-gfp while pH 8 showed the least expression. The FSC-A data also confirmed

319   our previous findings and demonstrated the largest changes in cell size appear at the

320   lowest pH after exposure to nalidixic acid (Supplementary Figure S4B).

321   These data illustrate that following DNA damage pH homeostasis is impaired and,

322   consequently, affects RecA expression and downstream processes. These data also

323   reinforce the fact that the external pH, via homeostasis loss, leads to altered

324   morphological plasticity following DNA damage.

325

326   **Transcription of later induced SOS genes are repressed by an external pH of 5.2**

327   Autoproteolytic degradation of the LexA transcription factor is a key step in the

328   regulation and induction of the SOS response genes. To observe the induction of *lexA*

329   an ectopic *lexA* promoter *gfpmut2* fusion was used (*plexA-gfp*, Supplementary Table

330   S1) (36). The *plexA-gfp* system was investigated as outlined above for *recA-gfp*. The

331   general pattern is similar to *recA-gfp* with a maximum expression around pH 6 with

332   the following key differences: at pH 5 the *lexA* promoter activity is poorly induced

333   and declines from180 min to 300 min Induction of the *lexA* promoter at pH 6-8 shows

334   slightly sigmodial dynamics whereby induction accelerates to a maximum between

335   60-120 min whereas *recA* starts at maximum induction only slowing from 120 min

336   (Figure 2C). Thus we show that *lexA* promoter expression is strongly influenced by

337   the external pH with an optimal expression at pH 7.

338   The LexA protein is known to have asymmetric affinity to the heterogeneous SOS

339   operator sequences and as such different genes are induced at varying LexA

340   concentrations (37). As pH equilibration occurs gradually following DNA damage we

341   hypothesised that the various SOS genes and their products could be differentially

342   affected (38). PolV mediated mutagenesis is detrimental to the fitness of most bacteria

343   and as a result the two SOS active components *umuD* and *umuC* of PolV are induced

344   late in the SOS response (39). To monitor the induction of *umuDC* an ectopic *umuDC*

345   promoter *gfpmut2* fusion was selected (*pumuDC-gfp*, Supplementary Table S1) (36).

346   The *pumuDC-gfp* system was tested as outlined above for *recA-gfp*. The fluorescent

347   signals of UmuDC-gfp start to increase after about 90 minutes of incubation,

348   confirming *umuDC* is induced later than *recA*. Further, following nalidixic acid

349   treatment *pumuDC* showed the highest and lowest induction in media at pH 6 and 5.2,

350   respectively (Supplementary Figure S5A). Analysis of FSC-A in the *umuDC*

351   *promoter* Gfpmut2 expressing cells at the indicated pH's revealed the same

16

352   filamentation patterns as *recA-gfp* expressing cells (Supplementary Figure S5B)

353   confirming the previous findings (Figure 2A). After adjustment of the Gfpmut2

354   fluorescent intensity signals to cell size, *pumuDC-gfp* showed the strongest induction

355   at pH 8 and practically no induction at 5.2 (Figure 2D), which is in contrast to *recA-*

356   *gfp* (Figure 2B). To directly compare the pH dependency of early and late induced

357   SOS genes, we plotted the 300 minutes after nalidixic acid exposure data points

358   across the permissible pH range (Figure 2E-F). These data indicate early induced

359   genes (*recA* and *lexA*) show maximum expression at pH 6 and 6.5 while late induced

360   genes (*umuD* and *umuC*) showed maximum expression over a broader pH-range (6-8)

361   (Figure 2D). Of the genes tested, only *recA* was found to be significantly induced at

362   pH 5.2.

363   Finally, the identical experimental setup allowed temporal comparisons of pH

364   equilibration against *recA-gfp, plexA-gfp* and *pumuDC-gfp* induction. Comparative

365   fluorescence density measurements (Figure 3A) clearly confirmed the earlier

366   induction of *recA-gfp* whose expression begins <30 minutes after exposure and up to

367   90 minutes before *umuDC-gfp* expression. The relative expression of *umuDC* is much

368   faster and plateaus at 180 minutes, similar to *recA-gfp*. *plexA-gfp* shows an

369   intermediate response, with a delayed start compared to *recA-gfp* but fast relative

370   expression that plateaus after 180 min of exposure to the antibiotic. Comparison of

371   intracellular pH and fluorescence density measurements also demonstrate induction of

372   early-induced SOS genes such as *recA* and *lexA* occurs whilst the pH is at or still near

373   physiological pH (Figure 3B-C). However, early expression for *recA* indicates that it

374   is exposed to a large gradient of pH's while later induced genes are expressed in an

375   environment where the pH is already approaching that of the external environment

376   (Figure 3D). Together, these results show that following DNA damage late induced

17

377   SOS genes are more susceptible to a reduction or loss of induction at low external

378   pHs whilst at pH 8 the opposite is observed.

379

380   **The biochemical activity of RecA is strongly dependent on pH**

381   The strong correlation between RecA expression, the strength of SOS induction and

382   their dependence on the external pH prompted us to investigate how pH affects

383   known biochemical activities of RecA. First, we used an electrophoresis mobility shift

384   assay to monitor the formation of RecA: DNA complexes. The binding of RecA to

385   fluorescently labelled ssDNA is strongly pH dependent with almost 10-fold higher

386   affinity observed at pH 5 compared to pH 8 (Figure 4A). This was accompanied also

387   by a change in the mobility of the RecA-ssDNA complexes, indicating a possible

388   conformational change of the filament (Supplementary Figure S6A). Second, a kinetic

389   study using stopped-flow allowed us to further investigate the DNA binding

390   properties of RecA at different pH's by monitoring increasing fluorescence of a

391   5´Cy3-labelled dT79 oligonucleotide after binding with ATP pre-incubated RecA

392   protein (Figure 4B-C and Supplementary Figure S6B) (20). Quantification of the

393   binding parameters confirmed that decreasing pH led to higher affinity (Figure 4B) as

394   well as a massive change in binding half-times (Figure 4C). Strikingly, the shift of pH

395   from 5 to 8 resulted in a more than 3000 times increase in half-times. In other words,

396   while at pH 5 it takes RecA less than one second to bind DNA, at pH 8 it needs

397   several minutes. Finally, we used a D-loop formation assay to directly correlate the

398   pH dependency of RecA-DNA binding with its ability to search for the homology

399   within the donor dsDNA plasmid. Indeed, reactions at lower pH resulted in maximal

400   activity, indicating that less RecA is required for the recombination reaction (Figure

401   4D and Supplementary Figure S6C). Based on altered SOS response we also elucidate

402   previously reported RecA coprotease activity on LexA repressor (40). Our

403   experiments show that RecA filaments stimulate LexA cleavage only at pH 6 in the

404   presence of ATP (Figure 5A).

405   To better understand the origins of transcriptional and RecA *in vitro* pH sensitivity we

406   chose to examine RecA K250R a cationic mutant found at the subunit-subunit

407   interface in RecA-ssDNA filaments that has shown pH dependent DNA three-strand

408   exchange as well as a slow general recombination DNA repair phenotype (41). We

409   hypothesised that this residue is responsible, at least partially, for the pH sensitivity

410   we had observed. Initially we used RecA K250R to show a significantly impaired

411   LexA autocatalytic activity (Figure 5B). As this mutant binds to ssDNA in a pH-

412   dependent manner (Supplementary Figure S7), similar to the wt protein, it is plausible

413   that impaired ATPase activity leads to a loss of coprotease activity. Taken together,

414   these data show that pH strongly affects the biochemical activities of RecA and are

415   remarkably similar to the *in vivo* SOS induction data.

416

417   **RecA K250 is important for SOS gene transcription at low pH**

418   Subsequently, we wished to understand if *recA K250R* altered the observed pH

419   depolarisation of the wild type strain. To do this the *recA K250R* strain

420   (Supplementary Table S1) was transformed with the pH sensitive reporter to create

421   *recA K250R GFPmut3** and intracellular pH changes following antibiotic exposure

422   were examined by flow cytometry (Figure 6A). We observed accelerated

423   depolarisation kinetics compared to wild type *recA* where equilibration with the

424   external media was achieved 1 hour earlier. This suggests that *recA K250R* was also

425   having an effect on the SOS genes, and particularly those induced late in the response.

426   Next we also monitored the SOS response of *recA K250R* using the GFP signal from

427   the *pumuDC-GFP* plasmid (*recA K250R pumuDC-gfp*) following DNA damage by

428   flow cytometry (Figure 6B). The transcriptional activity of *pumuDC* showed an

429   increase in pH sensitivity as compared to wt *recA*, with the greatest difference

430   between the two strains observed at pH 6-6.5 (Figure 6C), indicating that the K250

431   residue is responsible for increasing the transcriptional activity of *pumuDC* at lower

432   pH.

433

434   **Mutagenesis is strongly influenced by pH**

435   DNA damage-induced loss of pH homeostasis and corresponding changes in RecA

436   activities prompted us to hypothesise that genome stability may be affected over the

437   range of studied pH. The rate of mutagenesis was initially monitored using a lactose

438   reversion assay where the media was buffered across the permissible replicative range

439   in the *E. coli* FC40 strain (Supplementary Table S1) (42). Since the lactose reversion

440   assay detects frameshift mutations, base substitutions, and gene amplifications/

441   genome rearrangements, which in turn are dependent on a variety of SOS genes

442   including *recA, recBC, dinB, polB, and umuDC* (43), this allowed us to also monitor

443   the cumulative effect of the individual pathways in mutagenesis. The data illustrates

444   the strong influence external pH has over the rate of mutagenesis (Figure 7A). The

445   frequency of lactose reversions is close to zero at the extremes, pH 5 and 8, but

446   reaches a maximum between pH 6.5 and 7 (Figure 7B). Colonies formed at pH 7.5

447   arise due to lac-amplification rather than mutations as they occurred only gradually.

448   In contrast, most of the colonies at pH 6.5 and 7 form relatively quickly over the first

449   few days, suggesting point mutations are the predominant mechanism (44). These

450   data demonstrate how the external environment could affect the rate of mutagenesis in

451   niches of different pH.

20

452 Subsequently, we examined the pH dependency of a forward mutation assay as

453 opposed to the lactose reverse mutation assay. We used UV to directly induce DNA

454 damage and increase mutagenesis (Figure 7C), since all antibiotic minimum

455 inhibitory concentration assays tested showed pH dependency (Figures S8A-H). In

456 this case mutagenesis showed pH dependency with an observed minimum at pH 6 and

457 a maximum at pH 8. We concluded that mutagenesis is significantly influenced by pH

458 but that the specific stimuli the bacteria are exposed to alter the response. In our

459 examples, the lactose reversion assay, which is dependent on both entering into the

460 stationary phase and the DNA damage response results in the highest mutational

461 frequency from pH 6.5-7 whilst when only the SOS response is required the lowest

462 frequencies were found at pH 6.

463 To explain the differences in mutagenesis over the viable pH range for *E. coli* we

464 hypothesised that bacterial viability was pH dependent. We used propidium iodide

465 (PI) staining to monitor bacterial viability whereby PI enters the bacteria only upon

466 loss of membrane integrity. The results showed that the bacteria lose membrane

467 integrity at acidic pH after nalidixic acid exposure, whereas at pH 7-8 the membranes

468 of the bacteria remain impermeable to PI (Figure 7D). An identical experiment using

469 a *recA* mutant showed the loss of membrane permeability at low pH was significantly

470 dependent on *recA* (Figure 7E). Strikingly, at pH 8, where we recorded the highest

471 number of rifampicin resistant mutants there was both the lowest PI staining and

472 highest transcription of *pumuDC-gfp*. Additionally we investigated viability using a

473 classical colony forming survival assay (Supplementary Figure. S9), however, we

474 observed large variations at and after two hours that prevented any interpretation of

475 the significance of external pH.

476   Together our results clearly demonstrate that the environmental pH where bacteria

477   and antibiotics meet plays a significant role in antibiotic resistance development. This

478   appears to occur due to proton equilibration across the plasma membrane so that the

479   intracellular pH becomes that of the environment. This pH change subsequently

480   affects many downstream processes of the SOS DNA damage response system

481   ultimately leading to pH-dependent mutagenesis.

482

Discussion

In this work we aimed to understand the physiological consequences of environmental pH on the SOS response. We initially discovered, in response to the DNA-damaging antibiotic nalidixic acid, a failure of pH homeostasis in the bacterial population. This failure occurred in a controlled fashion over several hours as the cytoplasmic pH equilibrated with the extracellular pH environment. Subsequently, we showed the pH of the external media affects the strength of induction of the SOS genes *recA*, *lexA* and *umuDC*, and the rate of mutagenesis resulting in antibiotic resistant mutants. We also examined how pH affects the biochemical function of the RecA protein *in vitro* and show that at pH 8 binding of ssDNA was severely compromised, a finding which correlates well with the *in vivo* weak induction of *recA*. Additionally, we found that RecA K250, a pH sensitive residue in RecA, was partially responsible for RecA inducing *pumuDC-gfp* expression and essential up to a pH of 6.5. Taken together our results indicate that the pH of the surrounding environment can influence and enhance mutagenesis and thus accelerate antibiotic resistance development (Figure 8). We also suggest that pH depolarisation across the inner membrane could be a mechanism whereby bacteria directly sense the environmental pH following a lethal challenge to their DNA integrity. By this mechanism the environmental pH would automatically be sensed by all intracellular components including all translated proteins.

Environmental pH influences antibiotic resistance development

Specifically, our findings show the following pH-dependent responses to nalidixic acid treatment: At an external pH of 5.2 genetic instability is not detectable. This could be explained by the lack of *pumuDC* transcription and significant loss of membrane integrity. The primary survival response at this pH appears to be filamentation. As the external pH increases, membrane integrity improves so that it is

508 roughly the same as before the antibiotic was applied at pH's 7 and 8, at the same

509 time the transcriptional activity of the genes studied increases, increasing the

510 probability that translesion polymerases will be active. This could explain the

511 increased genome instability seen at the higher pH's. These increases in genome

512 instability at pH's above 6.5 also imply that the development of resistance to

513 antibiotics will be increased under these circumstances.

514 **The activities of RecA are sensitive to pH**

515 Early transcriptional activity leads RecA to be exposed to all possible pH's from

516 homeostatic to environmental pH. Previous *in vitro* studies have shown pH 6.2 is

517 optimal for stable RecA filamentation on ssDNA (45). Experiments comparing the

518 binding of SSB protein and RecA on ssDNA at pH's 7.5 and 6.2 showed the lower pH

519 greatly favoured RecA over SSB (46). DNA independent hydrolysis of ATP was

520 significant at pH 6 whilst undetectable at pH 7 (47). More recent work has

521 demonstrated both RecA nucleation and subsequent filament extension on SSB-

522 ssDNA complexes are strongly pH dependent, where pH 6.5, the lowest examined

523 pH, gave the highest nucleation and filamentation rates (48). We also found pH

524 dependencies regarding RecA's interaction with ssDNA. Affinity was strongest and

525 rate of binding fastest at pH 5 and became respectively weaker and slower as pH

526 increased. Ultimately we discovered almost no D-loop formation at pH 8 with the

527 implication that recombination is unlikely to occur *in vivo* once the intracellular pH

528 reaches 8. Optimal D-loop formation was seen at pH's 6-7 indicating that

529 recombination could potentially be an important resistance development mechanism

530 at these pH's. The origins of the pH sensitivity have been postulated to involve an

531 electrostatic interaction between the negatively charged core domain of one RecA

532 with the positively charged N-terminal domain of the next (49). Accordingly, we

24

533   examined the effect of the K250R RecA residue predicted to be involved in inter-

534   protein interactions. We found this mutant to be highly influenced by pH, this was

535   most clearly evident at pH 6 when compared to the wild-type, here there was a

536   significant reduction in LexA degradation and no expression of *umuDC*. We

537   conclude, therefore, that K250 and monomer-monomer interactions are important at

538   low pH and influential up to pH 7.5.

539   **A controlled loss of pH homeostasis**

540   The kinetic profile of proton depolarisation after DNA damage indicates how the

541   mechanism may proceed. The observed process contrasts with a physical breach of

542   the membrane which results in a near instantaneous pH equilibration. Indeed, even a

543   rapid shift in external pH without exposure to DNA damaging agents, for example, a

544   shift from 7.5 to 5.5 can result in an intracellular pH shift immediately to 6, with a

545   biphasic recovery beginning after 10 seconds and most of the physiological pH

546   recouped after 30 seconds, the remaining being recovered over the next 4 minutes

547   (24). Based on our data we concluded, therefore, that the observed mechanism did not

548   involve any rapid disruption of the inner membrane, temporary or permanent, but a

549   gradual and controlled loss of pH homeostasis.

550   The bacterium expends considerable resources in maintaining pH homeostasis and

551   optimal internal environment for the metabolism of the cell (50). However, our data

552   point to situations where the loss of homeostasis and thereby direct environmental

553   sensing of pH may be an advantage. As such the pHs used for the study of bacterial

554   proteins outside of the homeostatic range of 7.5-7.7 may be biologically relevant in

555   such cases. In an optimal environment the maintenance of ion gradients, to generate a

556   pmf, is important for energy production. However, under DNA damaging conditions,

557   it could be an advantage for the cell to enter a state of persistence, a dormant

558   condition where energetic processes are reduced to a minimum. Recently, dependency

559   between intracellular ATP concentrations and persister cell formation has been

560   established (51). Following DNA damage we show that, in addition to the loss of

561    $\Delta\Psi$, the cell also suffers a loss of ΔpH thus greatly reducing the capacity of the

562   bacterium to generate ATP.

Dynamic bacterial morphology following filamentation

564   We found the reduction in bacterial filamentation after 1 hour of exposure to

565   Nalidixic acid surprising as we assumed that filamentation would continue until either

566   the DNA damage stress is removed or the bacterium succumbs to the stress. Yet,

567   recent work suggests cell division could be a response to severe DNA damage-

568   induced stress. In order for cell division to occur replication must be completed.

569   When irreparable damage occurs on one DNA strand this dooms the bacterium that

570   receives this permanently damaged chromosome but allows the other bacterium with

571   an undamaged chromosome to continue proliferation (52,53). Double strand breaks as

572   produced by inhibition of topoisomerase ligation activities as in the case for nalidixic

573   acid could lead to a serious impact on bacterial viability for both chromosomes. Yet it

574   was interesting to note that reducing cell size following filamentation correlated with

575   the start of the slow phase of bacterial killing attributed to the presence of persister

576   cells in response to an overwhelming challenge to DNA integrity. We see this time

577   point as a change of survival tactics to better suit a chronic challenge to DNA

578   integrity.

A low external pH environment leads to enhanced filamentation with implications for phagocytosis

581   Varying intracellular pH should lead to altered biochemical activities of the cellular

582   proteins. Filamentation, or morphological plasticity, is a physiological change seen in

583 bacteria in response to DNA damage. The mechanism involves many components but

584 initiation is caused by the SOS protein SulA. Specifically SulA binds FtsZ and

585 thereby inhibits polymerisation of FtsZ which would otherwise form a ring at mid-cell

586 and thus inhibits septation (54). Other constituents involved in filamentation are

587 proteins participating in cell membrane and cell wall synthesis. From our results, it is

588 clear the sum of the pH effects on these components together leads to longer filaments

589 at lower pH, specifically 5.2 and 6 whilst at pH 7 and 8 the filaments are shorter. It is

590 interesting to note in uropathogenic *E. coli* SulA is essential for pathogenesis in

591 immunocompetent hosts (55,56). It has been postulated an influx of neutrophils

592 following bacterial emergence from epithelial cells results in the phagocytosis of

593 bacillary forms of uropathogenic *E. coli* but not filamented forms. Filamented *E. coli*

594 appear to be resistant to phagocytosis and exposure to an acidic environment, such as

595 in macrophages leads to a stronger filamentation phenotype so if the bacterium

596 survives it is unlikely to be engulfed again.

597 In conclusion we find that the pH of the environment will significantly affect the

598 mechanisms of antibiotic resistance and the rate at which they occur in response to

599 antibiotic treatment.

References

1. EU, F.C. (2014), *Transatlantic Taskforce on Antimicrobial Resistance: Progress report May 2014*, pp. 1-86.

2. Brauner, A., Fridman, O., Gefen, O. and Balaban, N.Q. (2016) Distinguishing between resistance, tolerance and persistence to antibiotic treatment. *Nature Reviews Microbiology*, **14**, 320-330.

3. Kohanski, M.A., Dwyer, D.J., Hayete, B., Lawrence, C.A. and Collins, J.J. (2007) A common mechanism of cellular death induced by bactericidal antibiotics. *Cell*, **130**, 797-810.

4. Miller, C., Thomsen, L.E., Gaggero, C., Mosseri, R., Ingmer, H. and Cohen, S.N. (2004) SOS response induction by beta-lactams and bacterial defense against antibiotic lethality. *Science*, **305**, 1629-1631.

5. Michel, B. (2005) After 30 years of study, the bacterial SOS response still surprises us. *Plos Biology*, **3**, 1174-1176.

6. Courcelle, J., Khodursky, A., Peter, B., Brown, P.O. and Hanawalt, P.C. (2001) Comparative gene expression profiles following UV exposure in wild-type and SOS-deficient Escherichia coli. *Genetics*, **158**, 41-64.

7. Harms, A., Maisonneuve, E. and Gerdes, K. (2016) Mechanisms of bacterial persistence during stress and antibiotic exposure. *Science*, **354**, 1390-+.

8. Dorr, T., Vulic, M. and Lewis, K. (2010) Ciprofloxacin Causes Persister Formation by Inducing the TisB toxin in Escherichia coli. *Plos Biology*, **8**, -.

9. Unoson, C. and Wagner, E.G.H. (2008) A small SOS-induced toxin is targeted against the inner membrane in Escherichia coli. *Mol. Microbiol.*, **70**, 258-270.

10. Slonczewski, J.L., Fujisawa, M., Dopson, M. and Krulwich, T.A. (2009) Cytoplasmic pH Measurement and Homeostasis in Bacteria and Archaea. *Adv Microb Physiol*, **55**, 1-79.

11. Slonczewski, J.L., Rosen, B.P., Alger, J.R. and Macnab, R.M. (1981) pH homeostasis in Escherichia coli: measurement by 31P nuclear magnetic resonance of methylphosphonate and phosphate. *Proc Natl Acad Sci U S A*, **78**, 6271-6275.

12. Baba, T., Ara, T., Hasegawa, M., Takai, Y., Okumura, Y., Baba, M., Datsenko, K.A., Tomita, M., Wanner, B.L. and Mori, H. (2006) Construction of Escherichia coli K-12 in-frame, single-gene knockout mutants: the Keio collection. *Mol Syst Biol*, **2**, 2006 0008.

13. Thomason, L.C., Costantino, N. and Court, D.L. (2007) E. coli genome manipulation by P1 transduction. *Current protocols in molecular biology / edited by Frederick M. Ausubel ... [et al.]*, **Chapter 1**, Unit 1 17.

14. Warren, D.J. (2011) Preparation of highly efficient electrocompetent Escherichia coli using glycerol/mannitol density step centrifugation. *Anal Biochem*, **413**, 206-207.

15. Datsenko, K.A. and Wanner, B.L. (2000) One-step inactivation of chromosomal genes in Escherichia coli K-12 using PCR products. *Proc Natl Acad Sci U S A*, **97**, 6640-6645.

16. Crumplin, G.C. and Smith, J.T. (1975) Nalidixic acid: an antibacterial paradox. *Antimicrob Agents Chemother*, **8**, 251-261.

17. Barrett, C.M.L., Ray, N., Thomas, J.D., Robinson, C. and Bolhuis, A. (2003) Quantitative export of a reporter protein, GFP, by the twin-arginine translocation pathway in Escherichia coli. *Biochemical and Biophysical Research Communications*, **304**, 279-284.

18. Matulova, P., Marini, V., Burgess, R.C., Sisakova, A., Kwon, Y., Rothstein, R., Sung, P. and Krejci, L. (2009) Cooperativity of Mus81.Mms4 with Rad54 in the resolution of recombination and replication intermediates. *J Biol Chem*, **284**, 7733-7745.

19. Sebesta, M., Burkovics, P., Haracska, L. and Krejci, L. (2011) Reconstitution of DNA repair synthesis in vitro and the role of polymerase and helicase activities. *DNA Repair (Amst)*, **10**, 567-576.

20. Taylor, M.R., Spirek, M., Chaurasiya, K.R., Ward, J.D., Carzaniga, R., Yu, X., Egelman, E.H., Collinson, L.M., Rueda, D., Krejci, L. *et al.* (2015) Rad51 Paralogs Remodel Pre-synaptic Rad51 Filaments to Stimulate Homologous Recombination. *Cell*, **162**, 271-286.

21. MuLler-Hill, B. and Kania, J. (1974) Lac repressor can be fused to [beta]-galactosidase. *Nature*, **249**, 561-563.

22. Drlica, K., Hiasa, H., Kerns, R., Malik, M., Mustaev, A. and Zhao, X.L. (2009) Quinolones: Action and Resistance Updated. *Curr Top Med Chem*, **9**, 981-998.

23. Erental, A., Sharon, I. and Engelberg-Kulka, H. (2012) Two programmed cell death systems in Escherichia coli: an apoptotic-like death is inhibited by the mazEF-mediated death pathway. *PLoS Biol*, **10**, e1001281.

24. Wilks, J.C. and Slonczewski, J.L. (2007) pH of the cytoplasm and periplasm of Escherichia coli: rapid measurement by green fluorescent protein fluorimetry. *J Bacteriol*, **189**, 5601-5607.

25. Nugent, S.G., Kumar, D., Rampton, D.S. and Evans, D.F. (2001) Intestinal luminal pH in inflammatory bowel disease: possible determinants and implications for therapy with aminosalicylates and other drugs. *Gut*, **48**, 571-577.

26. Tenaillon, O., Skurnik, D., Picard, B. and Denamur, E. (2010) The population genetics of commensal Escherichia coli. *Nature Reviews Microbiology*, **8**, 207-217.

27. Yang, L., Wang, K.J., Li, H., Denstedt, J.D. and Cadieux, P.A. (2014) The Influence of Urinary pH on Antibiotic Efficacy Against Bacterial Uropathogens. *Urology*, **84**.

28. Canton, J., Khezri, R., Glogauer, M. and Grinstein, S. (2014) Contrasting phagosome pH regulation and maturation in human M1 and M2 macrophages. *Mol Biol Cell*, **25**, 3330-3341.

29. Butala, M., Zgur-Bertok, D. and Busby, S.J. (2009) The bacterial LexA transcriptional repressor. *Cellular and molecular life sciences : CMLS*, **66**, 82-93.

30. Justice, S.S., Garcia-Lara, J. and Rothfield, L.I. (2000) Cell division inhibitors SulA and MinC/MinD block septum formation at different steps in the assembly of the Escherichia coli division machinery. *Mol. Microbiol.*, **37**, 410-423.

31. Trusca, D., Scott, S., Thompson, C. and Bramhill, D. (1998) Bacterial SOS checkpoint protein SulA inhibits polymerization of purified FtsZ cell division protein. *Journal of Bacteriology*, **180**, 3946-3953.

32. Mukherjee, A., Cao, C.N. and Lutkenhaus, J. (1998) Inhibition of FtsZ polymerization by SulA, an inhibitor of septation in Escherichia coli. *Proceedings of the National Academy of Sciences of the United States of America*, **95**, 2885-2890.

33. Volkmer, B. and Heinemann, M. (2011) Condition-Dependent Cell Volume and Concentration of Escherichia coli to Facilitate Data Conversion for Systems Biology Modeling. *Plos One*, **6**.

34. Patel, M., Jiang, Q.F., Woodgate, R., Cox, M.M. and Goodman, M.F. (2010) A new model for SOS-induced mutagenesis: how RecA protein activates DNA polymerase V. *Crit Rev Biochem Mol*, **45**, 171-184.

35. Renzette, N., Gumlaw, N., Nordman, J.T., Krieger, M., Yeh, S.P., Long, E., Centore, R., Boonsombat, R. and Sandler, S.J. (2005) Localization of RecA in Escherichia coli K-12 using RecA-GFP. *Mol Microbiol*, **57**, 1074-1085.

36. Friedman, N., Vardi, S., Ronen, M., Alon, U. and Stavans, J. (2005) Precise temporal modulation in the response of the SOS DNA repair network in individual bacteria. *PLoS Biol*, **3**, e238.

37. Lewis, L.K., Harlow, G.R., Greggjolly, L.A. and Mount, D.W. (1994) Identification of High-Affinity Binding-Sites for Lexa Which Define New DNA Damage-Inducible Genes in Escherichia-Coli. *Journal of Molecular Biology*, **241**, 507-523.

38. Goodman, M.F., McDonald, J.P., Jaszczur, M.M. and Woodgate, R. (2016) Insights into the complex levels of regulation imposed on Escherichia coli DNA polymerase V. *DNA Repair*, **44**, 42-50.

39. Sommer, S., Boudsocq, F., Devoret, R. and Bailone, A. (1998) Specific RecA amino acid changes affect RecA-UmuD ' C interaction. *Mol. Microbiol.*, **28**, 281-291.

40. Giese, K.C., Michalowski, C.B. and Little, J.W. (2008) RecA-dependent cleavage of LexA dimers. *Journal of Molecular Biology*, **377**, 148-161.

41. Cox, J.M., Li, H., Wood, E.A., Chitteni-Pattu, S., Inman, R.B. and Cox, M.M. (2008) Defective dissociation of a "Slow" RecA mutant protein imparts an Escherichia coli growth defect. *Journal of Biological Chemistry*, **283**, 24909-24921.

42. Cairns, J. and Foster, P.L. (1991) Adaptive Reversion of a Frameshift Mutation in Escherichia-Coli. *Genetics*, **128**, 695-701.

43. Frisch, R.L., Su, Y., Thornton, P.C., Gibson, J.L., Rosenberg, S.M. and Hastings, P.J. (2010) Separate DNA Pol II- and Pol IV-Dependent Pathways of Stress-Induced Mutation during Double-Strand-Break Repair in Escherichia coli Are Controlled by RpoS. *Journal of Bacteriology*, **192**, 4694-4700.

44. Rosenberg, S.M. and Hastings, P.J. (2004) Adaptive point mutation and adaptive amplification pathways in the Escherichia coli Lac system: Stress responses producing genetic change. *Journal of Bacteriology*, **186**, 4838-4843.

45. Mcentee, K., Weinstock, G.M. and Lehman, I.R. (1981) Binding of the Reca Protein of Escherichia-Coli to Single-Stranded and Double-Stranded DNA. *Journal of Biological Chemistry*, **256**, 8835-8844.

729   46.   Pinsince, J.M., Muench, K.A., Bryant, F.R. and Griffith, J.D. (1993) 2 Mutant Reca Proteins
730   Possessing Ph-Dependent Strand Exchange Activity Exhibit Ph-Dependent Presynaptic
731   Filament Formation. *Journal of Molecular Biology*, **233**, 59-66.
732   47.   Muench, K.A. and Bryant, F.R. (1990) An Obligatory Ph-Mediated Isomerization on the
733   [Asn-160]Reca Protein-Promoted DNA Strand Exchange-Reaction Pathway. *Journal of*
734   *Biological Chemistry*, **265**, 11560-11566.
735   48.   Bell, J.C., Plank, J.L., Dombrowski, C.C. and Kowalczykowski, S.C. (2012) Direct imaging
736   of RecA nucleation and growth on single molecules of SSB-coated ssDNA. *Nature*, **491**, 274-
737   U144.
738   49.   Kim, S.H., Park, J., Joo, C., Kim, D. and Ha, T. (2015) Dynamic Growth and Shrinkage
739   Govern the pH Dependence of RecA Filament Stability. *Plos One*, **10**.
740   50.   Krulwich, T.A., Sachs, G. and Padan, E. (2011) Molecular aspects of bacterial pH sensing and
741   homeostasis. *Nature Reviews Microbiology*, **9**, 330-343.
742   51.   Shan, Y., Gandt, A.B., Rowe, S.E., Deisinger, J.P., Conlon, B.P. and Lewis, K. (2017) ATP-
743   Dependent Persister Formation in Escherichia coli. *Mbio*, **8**.
744   52.   Laureti, L., Demol, J., Fuchs, R.P. and Pages, V. (2015) Bacterial Proliferation: Keep
745   Dividing and Don't Mind the Gap. *Plos Genetics*, **11**.
746   53.   Lopes, M., Foiani, M. and Sogo, J.M. (2006) Multiple mechanisms control chromosome
747   integrity after replication fork uncoupling and restart at irreparable UV lesions. *Molecular*
748   *Cell*, **21**, 15-27.
749   54.   Justice, S.S., Hunstad, D.A., Cegelski, L. and Hultgren, S.J. (2008) Morphological plasticity
750   as a bacterial survival strategy. *Nature Reviews Microbiology*, **6**, 162-168.
751   55.   Horvath, D.J., Li, B.R., Casper, T., Partida-Sanchez, S., Hunstad, D.A., Hultgren, S.J. and
752   Justice, S.S. (2011) Morphological plasticity promotes resistance to phagocyte killing of
753   uropathogenic Escherichia coli. *Microbes Infect*, **13**, 426-437.
754   56.   Justice, S.S., Hunstad, D.A., Seed, P.C. and Hultgren, S.J. (2006) Filamentation by
755   Escherichia coli subverts innate defenses during urinary tract infection. *Proceedings of the*
756   *National Academy of Sciences of the United States of America*, **103**, 19884-19889.
757
758
759

760   **Figure 1.**


761

762

763

32
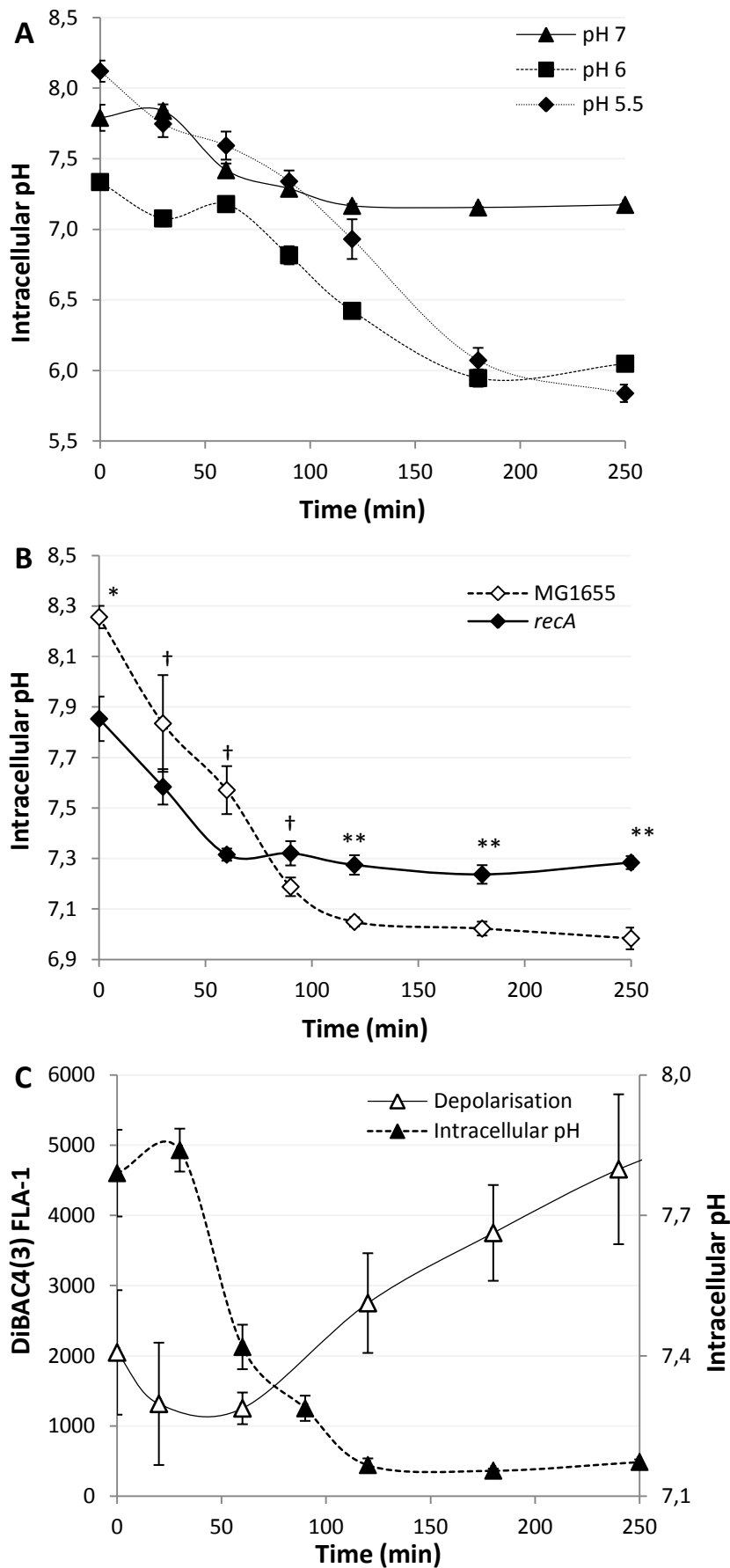
764   DNA damage leads to *recA* dependent loss of pH homeostasis. (**A-C**) The

765   cytoplasmic pH of *E. coli* was measured using calibrated GFPmut3* fluorescent

766   intensity measurements using flow cytometry following Nalidixic acid (100 µg/ml)

767   induced DNA damage at 0 min. (**A**) pH depolarisation was followed over four hours,

768   the extracellular media was buffered to 5.5, 6 and 7, as indicated on the graph. (**B**) pH

769   equilibration is not complete in a *recA* mutant following exposure to Nalidixic acid at

770   pH 7. (**C**) Intracellular pH equilibrates with the extracellular pH before electrical

771   polarity as measured by DiBAC4(3) following DNA damage in wild type *E. coli*. All

772   data points shown are mean ± s.e.m., *n* =4 (independent replicates). †p > 0.05, *p

773   ≤0.05, ** p ≤0.01 (t-test, two tail, unpaired equal variance).

774

775 **Figure 2.**


776

777

34

778

779

780

781
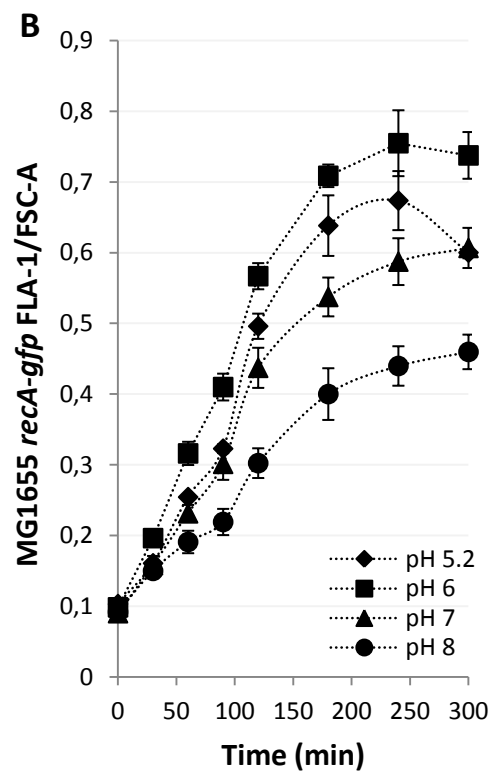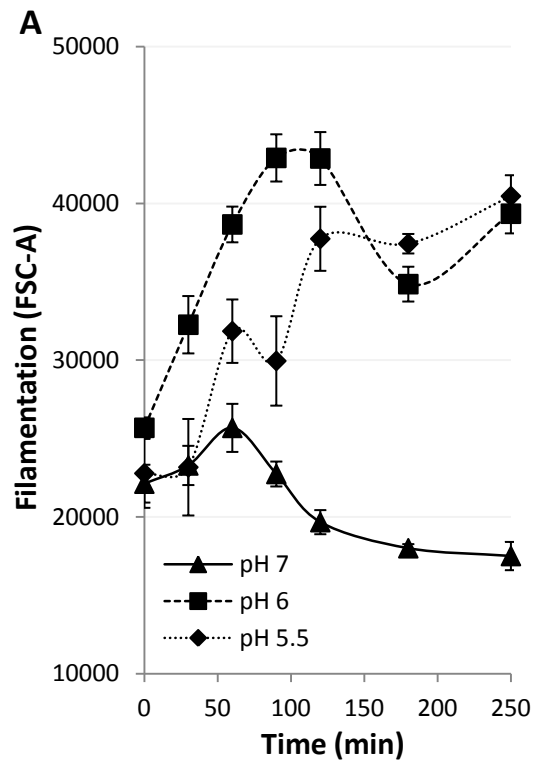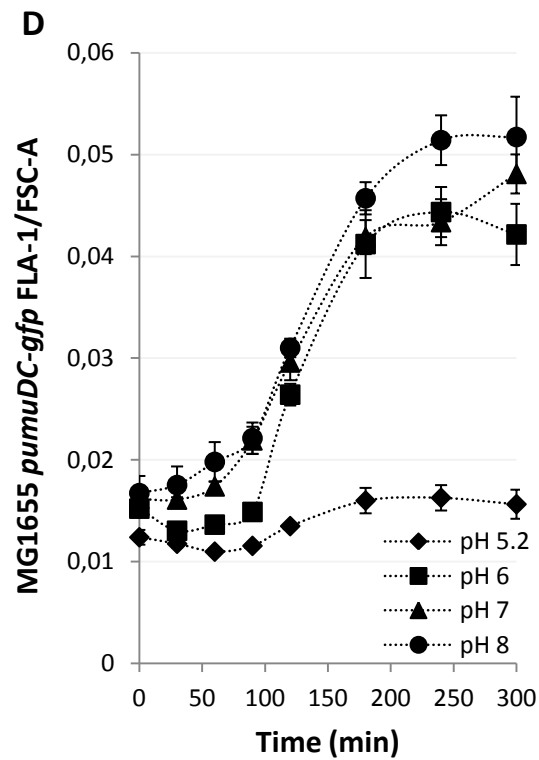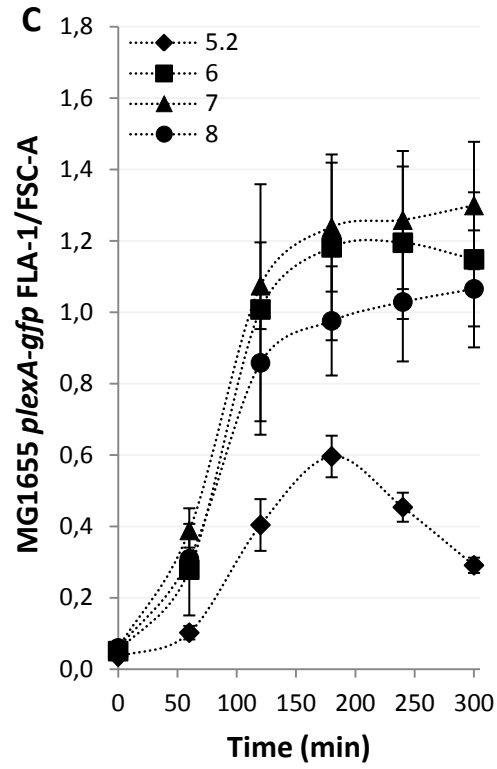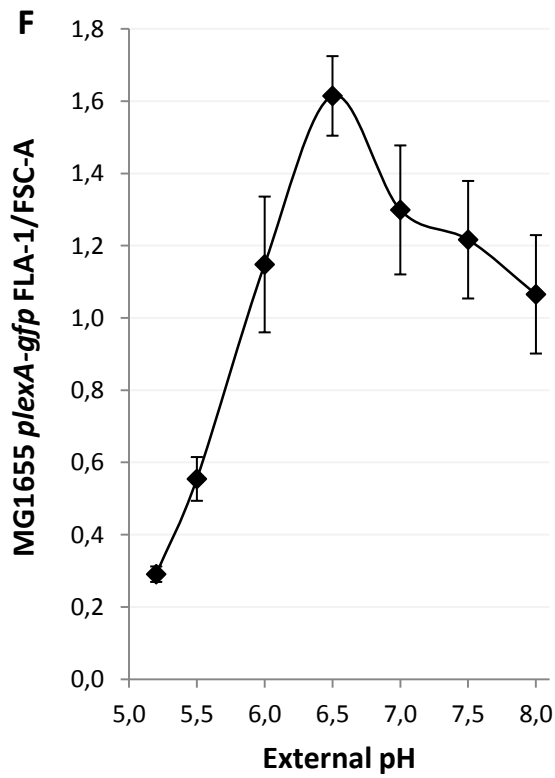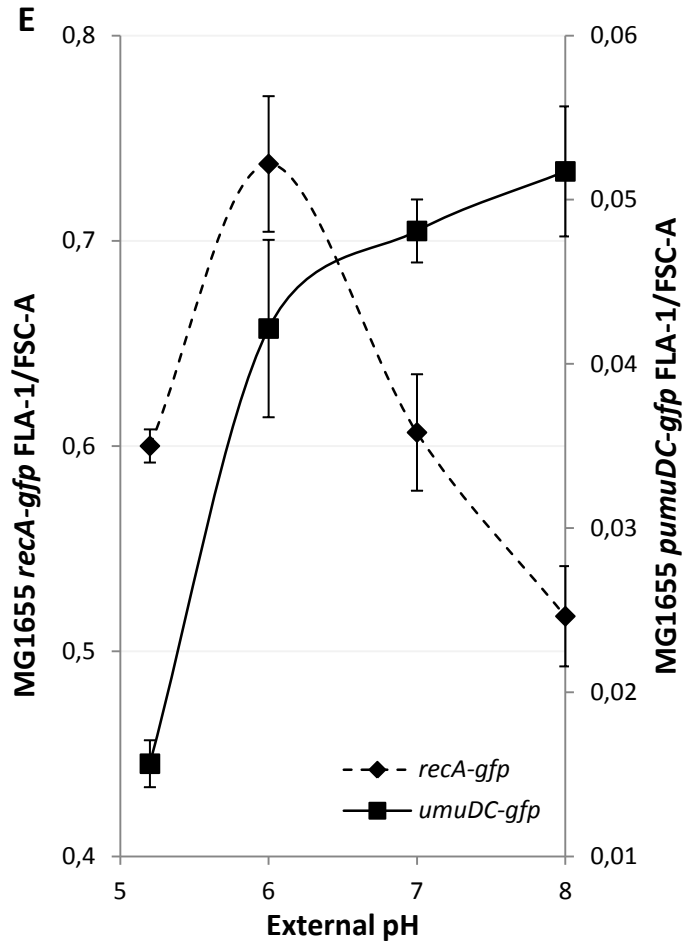
782 Proton depolarisation results in extracellular pH dependent affects on morphological

783 plasticity and transcription of SOS genes *recA, lexA* and *umuDC*. (**A-D**) DNA damage

784 was induced with Nalidixic acid (100 μg/ml) at 0 min and signals followed for 5

785 hours. (**A**) Kinetics and extent of filamentation, as defined by FSC-A, were followed

786 by flow cytometry in wild type *E. coli*. (**B-D**) The liquid media was buffered to pH

787 5.2, 6, 7 and 8 and the gfpmut2 signal followed by flow cytometry. GFP fusions

788 measured by fluorescence density measurements were (**B**) *recA-gfpmut2,* (**C**) *plexA -*

789 *gfpmut2,* (**D**) *pumuDC -gfpmut2*. (**E**) The pH dependence of *recA* and the *umuDC*

790 operon transcription following DNA damage (5 hours). (**F**) The pH dependence of

791 *recA* transcription following DNA damage (5 hours). All data points are mean ±

792 s.e.m., *n* =4 (independent replicates).

793

Figure 3.

798 The contrasting induction kinetics of SOS genes leads to different pH environments

799 for early and late genes. The media was buffered to pH 6 in all cases and DNA

800 damage induced by nalidixic acid (100 µg/ml) at time point 0. All GFP signals were

801 followed by flow cytometry at the indicated time points. (**A**) *recA* expression as

802 determined by the fluorescence signal of *recA-gfp* is quickly induced following DNA

803 damage as compared to *pumuDC-gfp*. (**B-D**) Intracellular pH and gene expression

804 levels were inferred from the fluorescence signals of GFP. (**B**) The immediate

805 induction of *recA-gfp* leads to significant induction occurring at homeostatic pH as

806 compared to genes induced at later time points. (**C**) The kinetics of *plexA-gfp*

807 induction leads to an intermediate situation where induction occurs mostly as the

808 intracellular pH is falling. (**D**) The slower induction of *pumuDC-gfp* results in the

809 induction occurring at non-homeostatic pHs.

810   **Figure 4.**

811

812

813

814

815

816
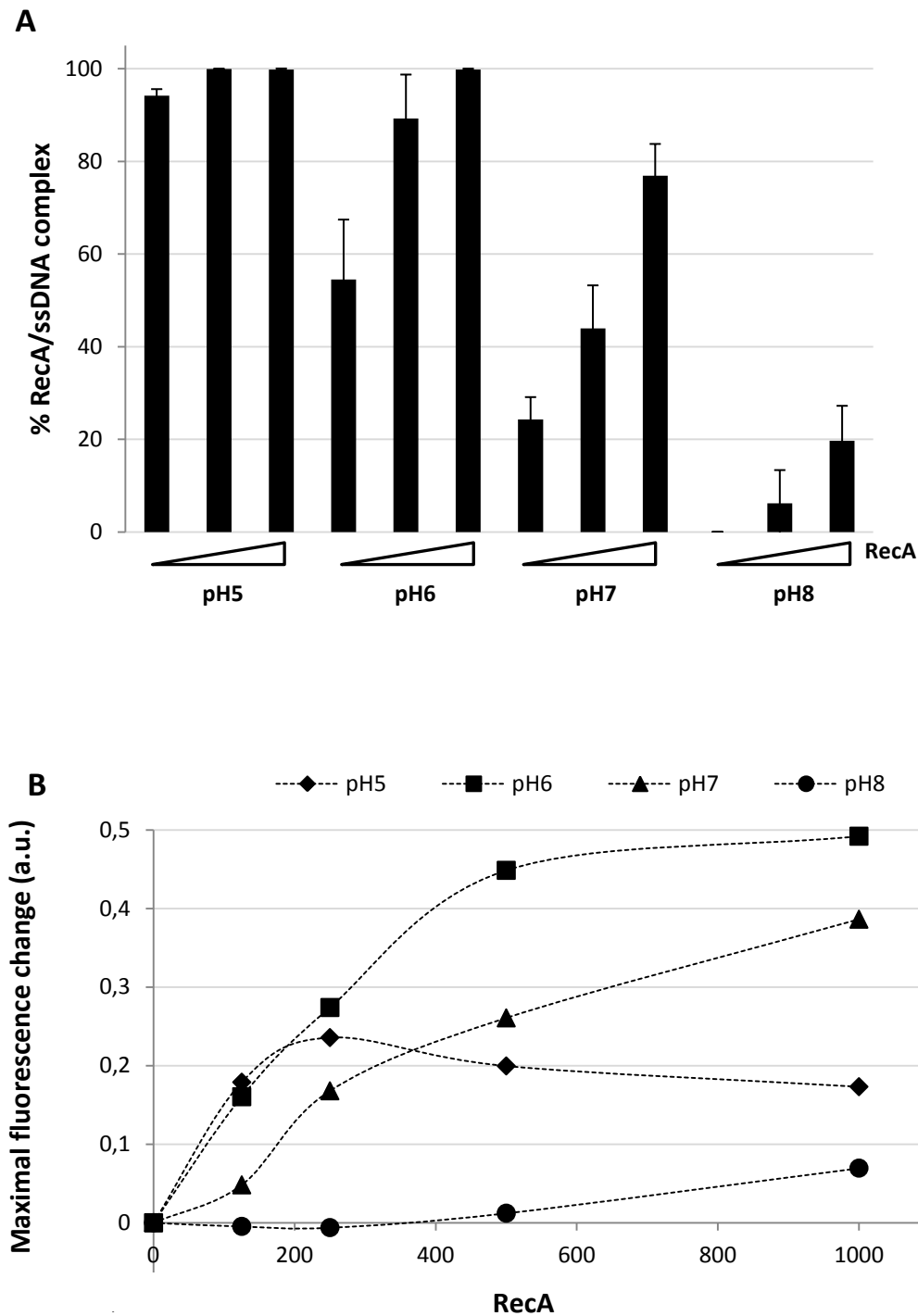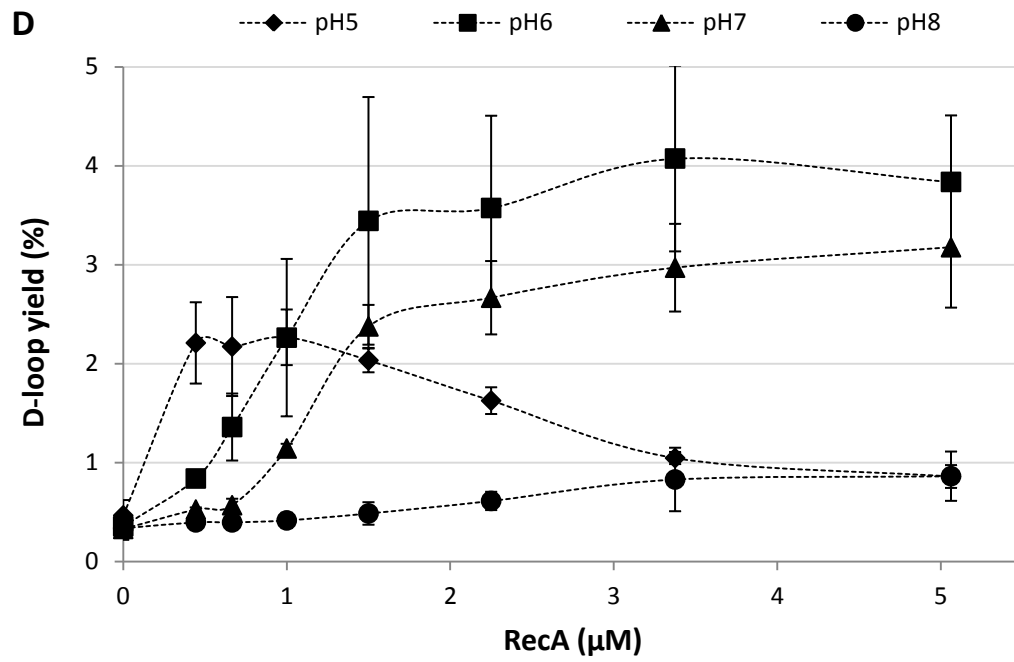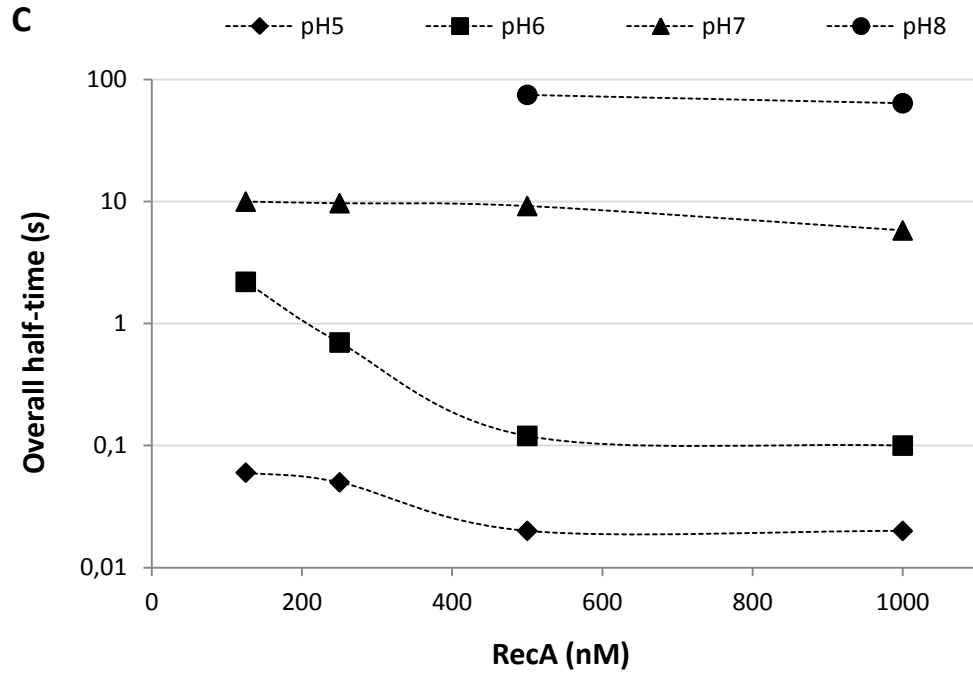
817   pH dramatically effects RecA biochemical activities. (**A**) The effect of pH on the

818   ssDNA binding activity of RecA by EMSA. (mean ± s.d. error bars, ($n = 3$)). (**B**) pH

819   dependency of RecA filament assembly by stopped-flow assay. Maximal change of

820   fluorescence is depicted. (**C**) Overall half-times of ssDNA binding. (**D**) Efficiency of

821   D-loop formation by RecA at various pH. (mean ± s.d. error bars, ($n = 3$)).

822 **Figure 5.**

823

824

825
826
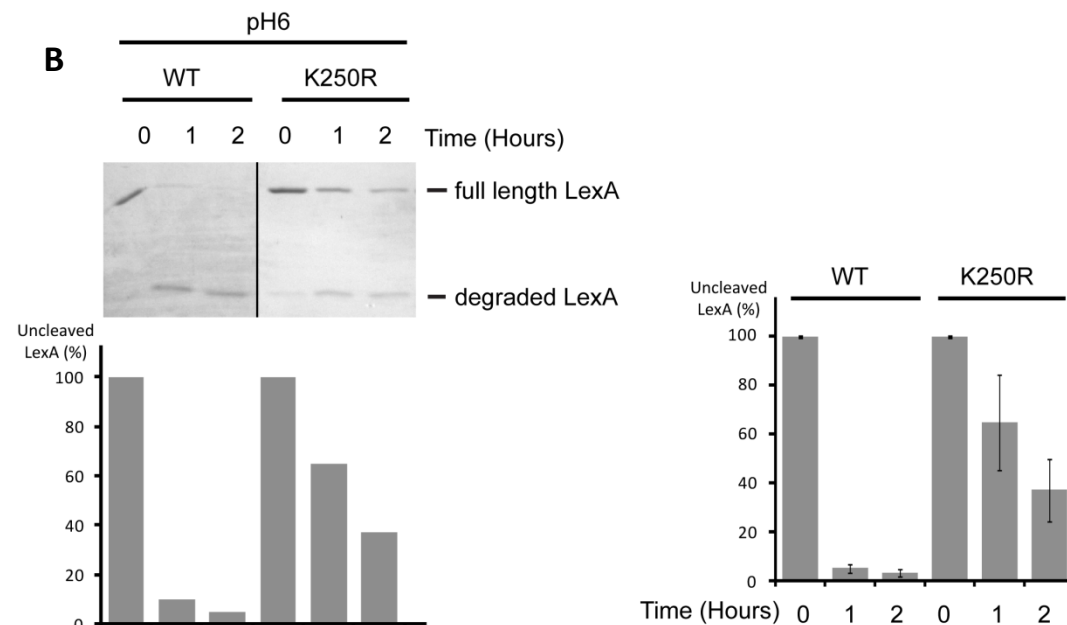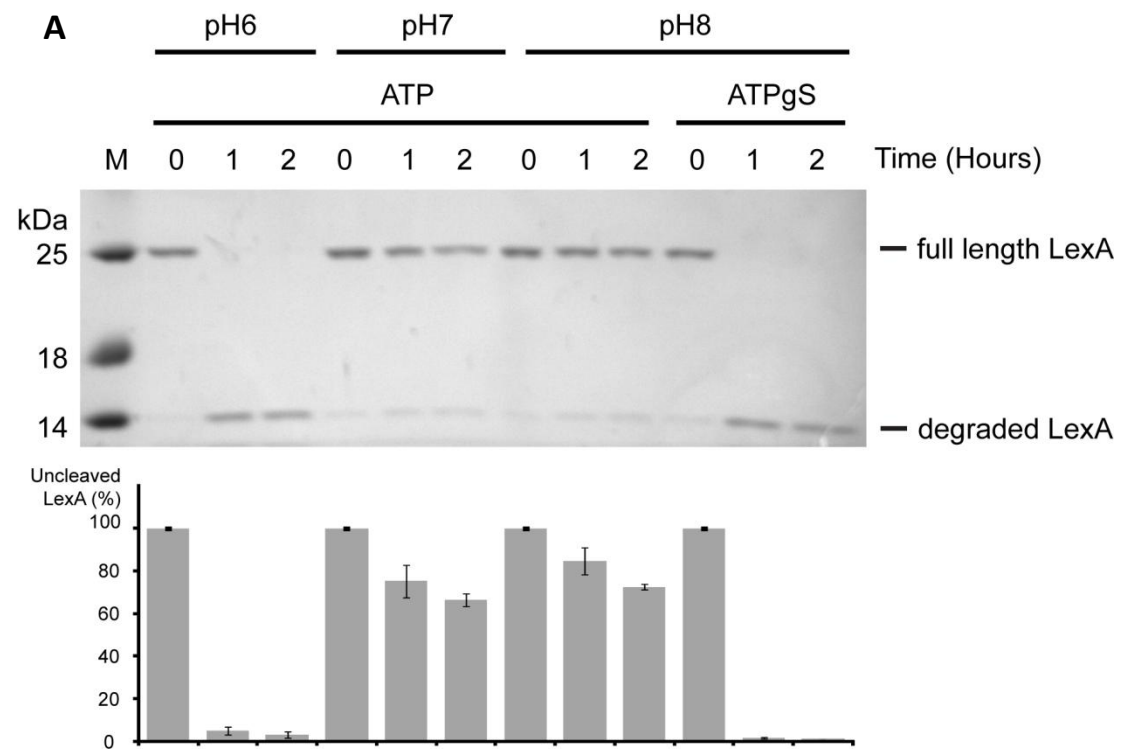
827   pH affects RecA co-protease activity on LexA cleavage. (**A**) The effect of pH on the

828   RecA co-protease activity on LexA cleavage (mean ± s.d. error bars, ($n = 3$)) in the

829   presence of ATP or ATPγS. (**B**) RecA K250R co-protease activity on LexA cleavage

830   (mean ± s.d. error bars, ($n = 3$)) in the presence of ATP and pH 6.

831

832   **Figure 6.**

833

835
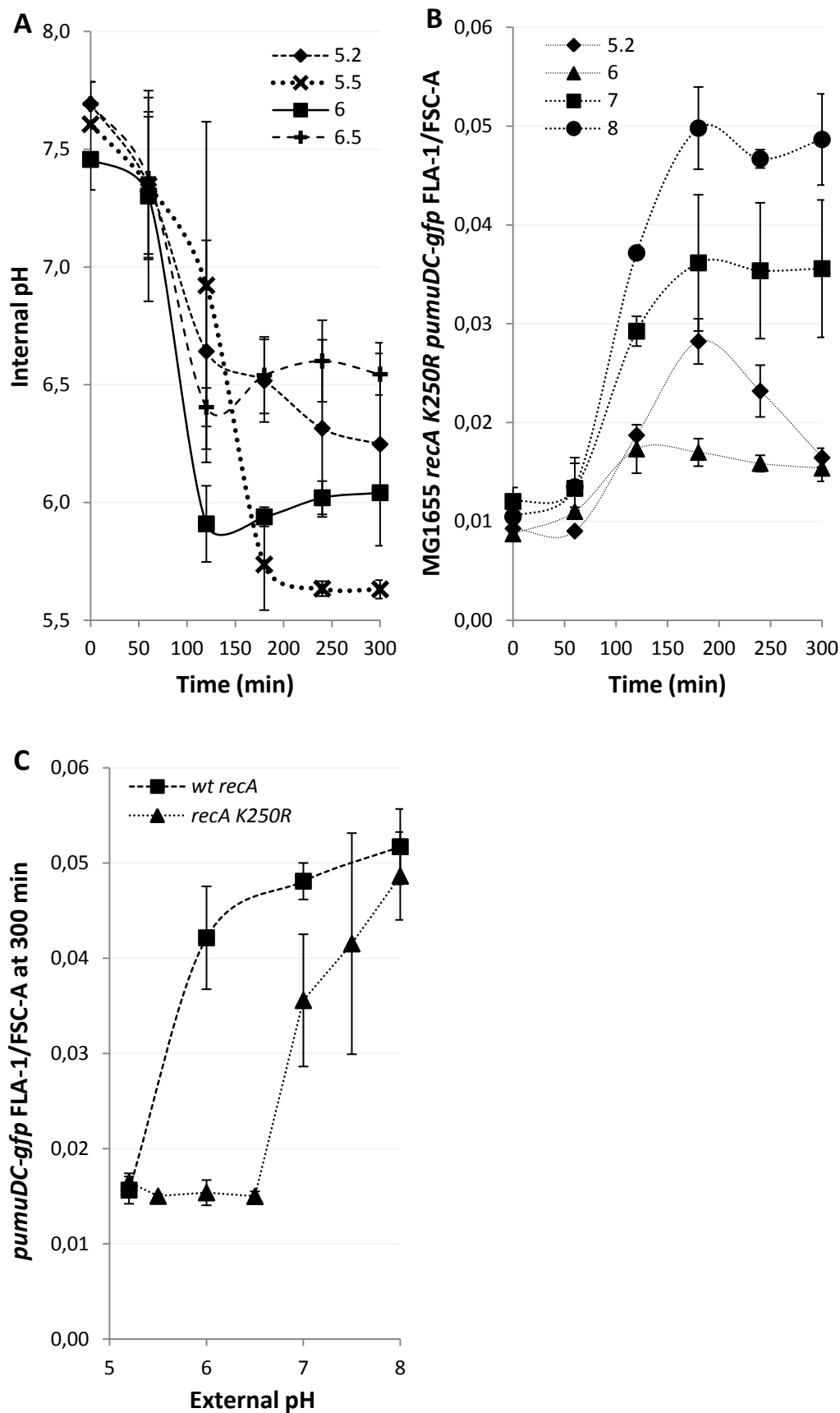
836   RecA K250 is responsible for increasing expression of late SOS genes at low pH. All

837   GFP signals were recorded using a flow cytometer. (**A-B**) DNA damage was induced

838   at time point 0 with nalidixic acid (100 μg/ml) and the GFP signals recorded at the

839   time points indicated. (**A**) pH equilibration with the external media over the viable *E.*

840   *coli* range is faster with RecA K250R than wt RecA. (**B**) The late induced operon

841   *umuDC* shows reduced expression at lower external pH's in a *recA* K250R

842   background. (**C**) The differences in expression are greatest at pH 6-6.5 where virtually

843   no expression is seen in the *recA* K250R background following 5 hours of exposure to

844   Nalidixic acid. For each data point the mean ± s.e.m. error bars is shown, ($n = 3$

845   independent replicates))

846 **Figure 7.**

847

848
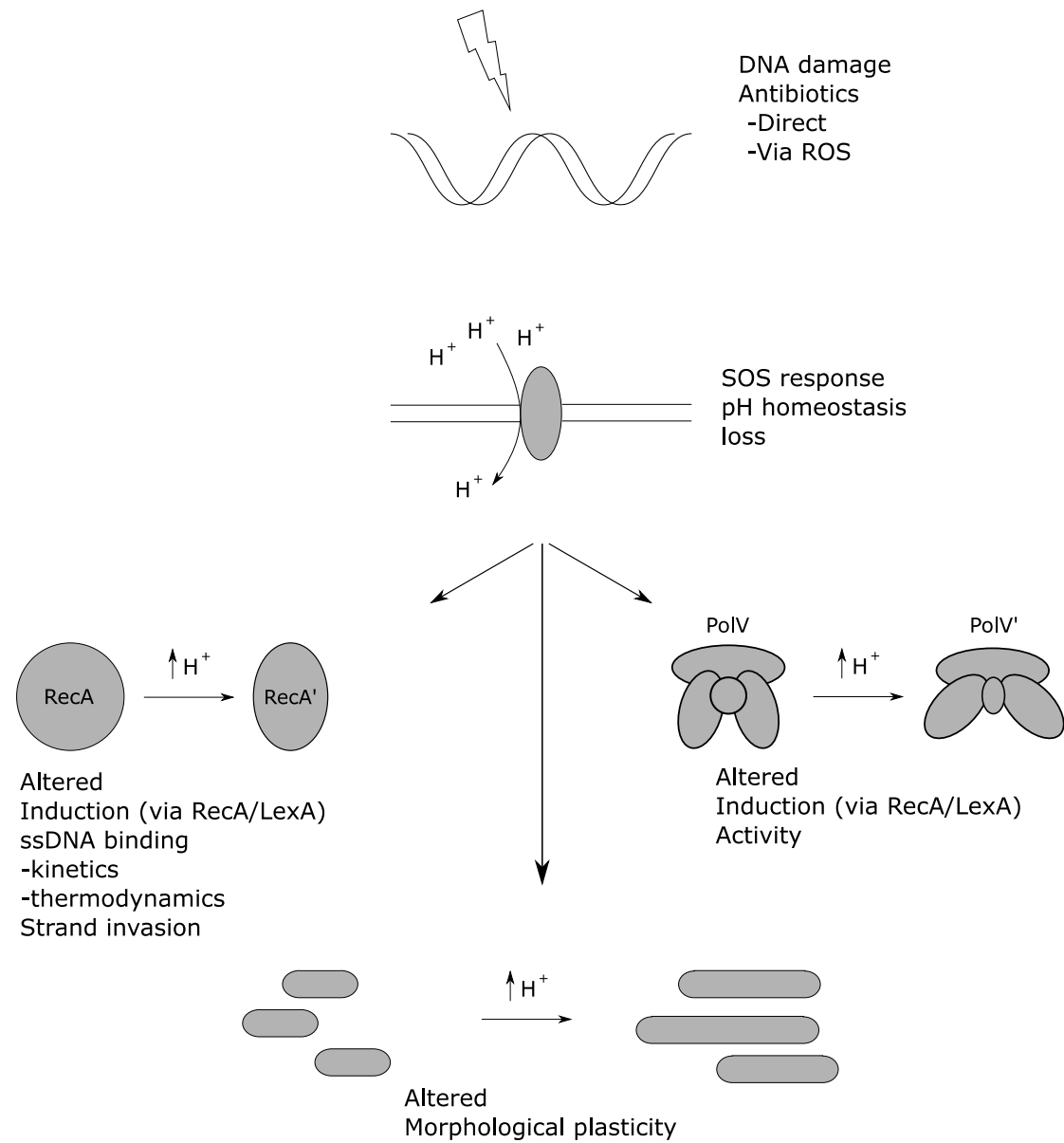
849

D

850

E

851
852
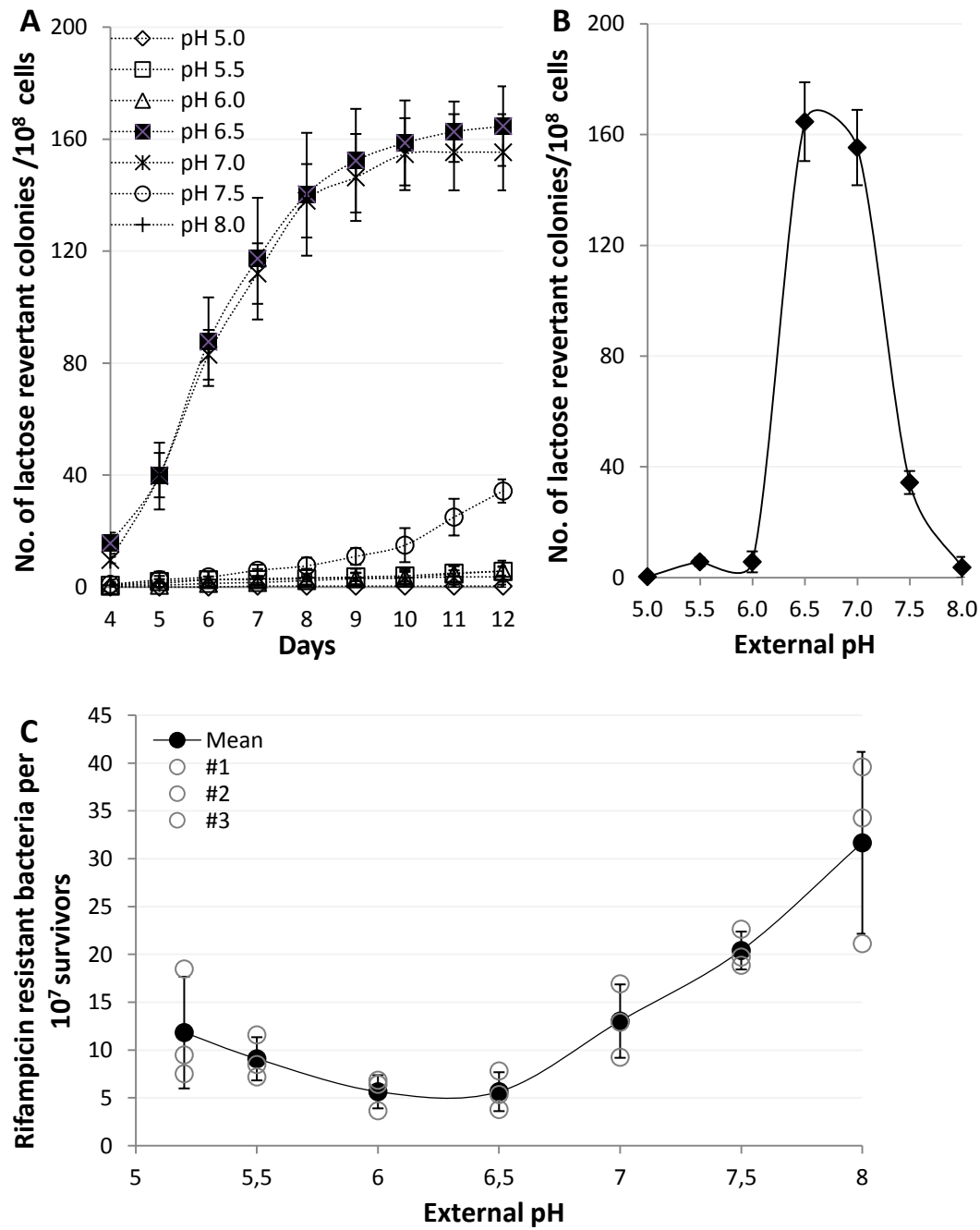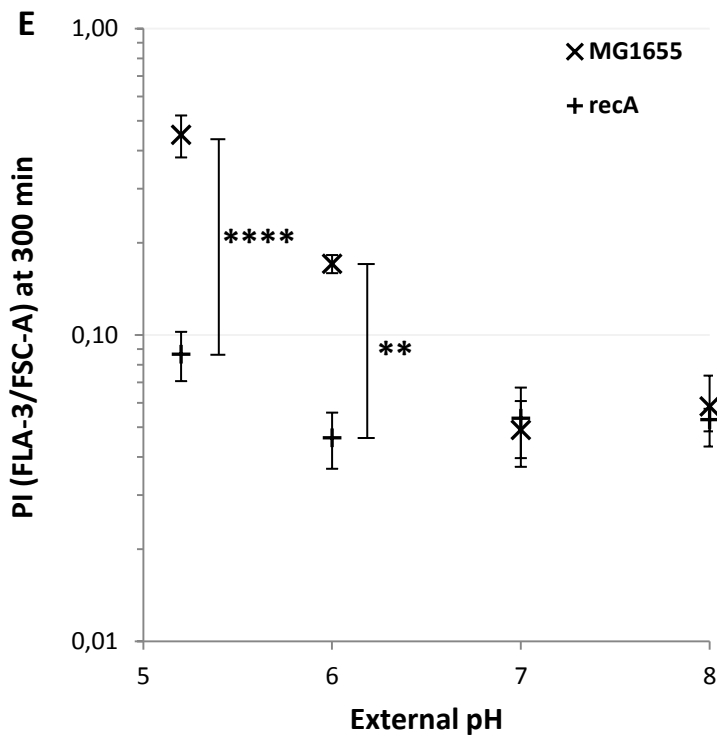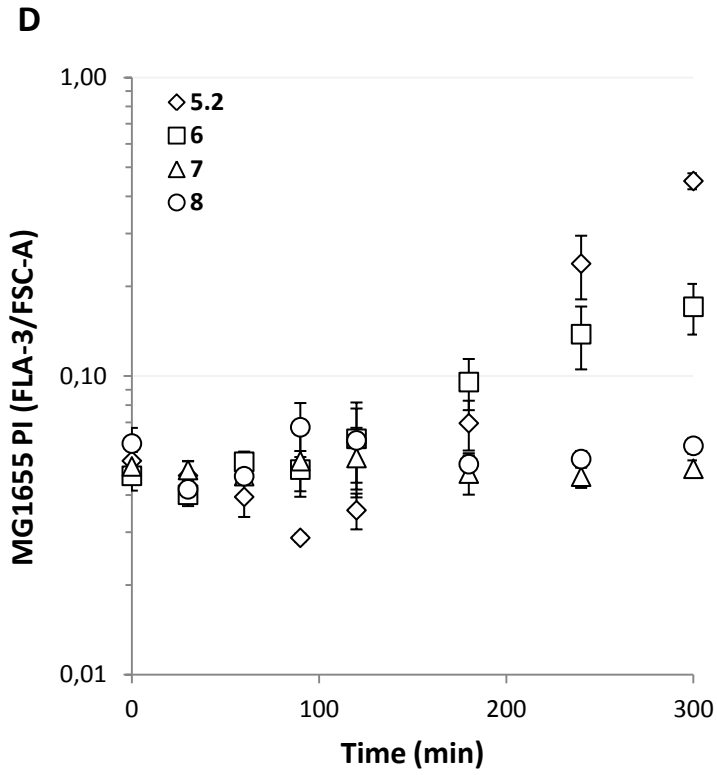
853   Extracellular pH strongly influences mechanisms of genetic resistance development

854   and membrane integrity. (**A-C**) For each data point the mean ± s.e.m. error bars is

855   shown, (*n* = 3 independent replicates). (**A**) A lactose reversion assay using *E. coli*

856   strain FC40, which cannot utilize lactose, when grown on minimal media plates with

857   lactose as the sole carbon source. Genetically resistant, reverted, populations appear

858   over several days and the rate is indicative of the rate of resistance development. (**B**)

859   A pH dependence profile after 12 days showing the total number of lactose reverted

860   colonies. (**C**) pH dependence of a forward UV induced rifampicin resistance assay.

861   Mean, filled circles ± standard deviation (n=3 (independent replicates), empty

862   circles). (**D-E**) DNA damage was induced by nalidixic acid (100 µg/ml). For each

863   data point the mean ± s.e.m. error bars is shown, (*n* = 4 independent replicates) (**D**)

864   The more acidic the environment the higher the level of membrane instability and

865   permeability. PI density staining following DNA damage induction with nalidixic

866   acid at time point 0 at the pH's and time points shown. (**E**) PI density staining after 5

867   hours of exposure to nalidixic acid shows that the membrane instability at acidic pH's

868   is *recA* dependent. ** p ≤0.01, **** p ≤0.0001 (t-test, two tail, unpaired equal

869   variance).

870

871 **Figure 8.**

DNA damage
Antibiotics
 -Direct
 -Via ROS

SOS response
pH homeostasis
loss

$\uparrow H^+$

RecA → RecA'

Altered
Induction (via RecA/LexA)
ssDNA binding
-kinetics
-thermodynamics
Strand invasion

PolV   PolV'

$\uparrow H^+$

Altered
Induction (via RecA/LexA)
Activity

$\uparrow H^+$

Altered
Morphological plasticity

872
873

874

875   Proposed working model of the flow of pH dependent events following DNA damage.

876   DNA damage, for example from exposure to antibiotics, results in the stimulation of

877   the SOS response. The SOS response results in a gradual loss of pH homeostasis, in

878   turn the proton depolarisation results in an altered biochemical environment touching

879   all biological processes. Here we specifically show *recA* induction, RecA's kinetics

880   and thermodynamics with regards to ssDNA and strand invasion are affected.

881   Additionally morphological plasticity and other downstream processes such as the

882   activity of TLS polymerases are affected.